JMEPEG
DOI: 10.1007/s11665-016-2421-9
©The Author(s). This article is published with open access at Springerlink.com
1059-9495/$19.00

Evolution of Globular Microstructure and Rheological Properties of Stellite™ 21 Alloy after Heating to Semisolid State

Krzysztof Piotr Sołek, Łukasz Rogal, and Platon Kapranos

(Submitted October 16, 2015; in revised form October 26, 2016)

Metal alloys can be successfully thixoformed in the partially liquid state if they display non-dendritic near-globular microstructures. The article presents the development of feedstock with such non-dendritic microstructure produced through the solid-state route of strain-induced melt-activated (SIMA) method, for a Stellite™ 21 alloy. Stellite™ alloys are a range of cobalt-chromium alloys designed for wear and corrosion resistance, currently shaped by casting, powder metallurgy or forging processes, but semisolid-state processing offers the possibility of a near-net-shaping method for these alloys. In this work, sprayformed followed by extrusion samples were heated to the temperature range at which the liquid and solid phases coexist in the material and spheroidal shape solid particles in a liquid matrix were obtained as required for semisolid processing. Microstructural investigations were carried out using scanning electron microscopy (SEM) in combination with energy-dispersive spectroscopy (EDS), with a further objective of analyzing the rheological properties of Stellite™ 21 alloy in the semisolid state, providing results to be used for identification of a processing window of temperature and viscosity ranges for thixoforming this alloy.

Keywords globular microstructure, rheological properties, Stellite™ alloys, scanning electron microscopy, thixoforming

1. Introduction

Recently, the development of a near-net-shape production technology that uses alloy feedstock in the semisolid state, referred to as thixoforming, has become the focus of a great deal of attention both from researchers in scientific institutions as well as industry. The initial concept of thixoforming was discovered by researchers of a group led by Prof. Merton Flemings at the Massachusetts Institute of Technology (Ref 1) and currently many aluminum and magnesium alloys parts manufactured using this production route have found industrial applications. From a technological point of view, such manufacturing processes have adapted forging (thixoforging) or casting (thixocasting) technologies and operate in the semisolid range.

Thixoforming is successfully used by a number of industries, such as automotive and consumer products in magnesium and aluminum alloys (Ref 2, 3). Using this technology, numerous electronic and automotive parts made of light metal alloys, such as laptop casings, suspension parts, car engine brackets and so forth, are produced (Ref 4).

Krzysztof Piotr Sołek, AGH University of Science and Technology, al. Mickiewicza 30, 30-059 Kraków, Poland; **Łukasz Rogal**, Institute of Metallurgy and Materials Science, PAS, ul. Reymonta 25, 30-059 Kraków, Poland; and **Platon Kapranos**, Department of Materials Science and Engineering, The University of Sheffield, Sir Robert Hadfield Building, Mappin Street, Sheffield S1 3JD, UK. Contact e-mail: ksolek@metal.agh.edu.pl.

However, thixoforming of high melting point alloys such as steel, copper, Stellite™ is still in the research stage. With such high melting point materials, many practical difficulties must be still overcome before manufacturing parts at the industrial level. Nevertheless, the interest in this area is great due to the many potential applications.

A number of different challenges in shaping high melting point alloys are currently under study, such as identification of the process conditions (Ref 5, 6), development of tool materials (Ref 7, 8) and heating and handling of feedstock (Ref 9).

The work presented here is a study of the microstructural development of non-dendritic feedstock of Stellite™ 21 alloy (previously known as Stellite™ 8) supplied after hot extrusion to be used in thixoforming carried out in the semisolid state. In the case of Stellite™ alloys, a low melting point eutectic, as shown in (Fig. 1), appears in the C-Co system and the solidus temperature of Stellite™ 21 alloy results directly from this system. The melting range of this alloy corresponds to a temperature range from 1295 to 1435 °C (Fig. 2); this large temperature difference between solidus and liquidus provides a nice process window for practical industrial applications. Additionally, in order to achieve better quality end products by thixoforming, it is important to have feedstock material with a near-globular, rather than a dendritic microstructure (Ref 10). Better quality of the products mainly means better their mechanical properties in comparison with classical casts. Materials with near-globular microstructure in the semisolid state behave thixotropically, i.e., they exhibit shear- and time-dependent viscosity (Ref 11), hence the name of this process. As a result of thixotropy phenomenon, a decrease in viscosity could be observed with the time of shearing.

But generally, an advantage in semisolid processing is the higher viscosity, what causes the laminar flow of metal alloys and production of parts displaying a lower number of defects in comparison with traditional, high-pressure die casting. Also, due to the fact that the flow of the slurry material is quite

Published online: 21 November 2016

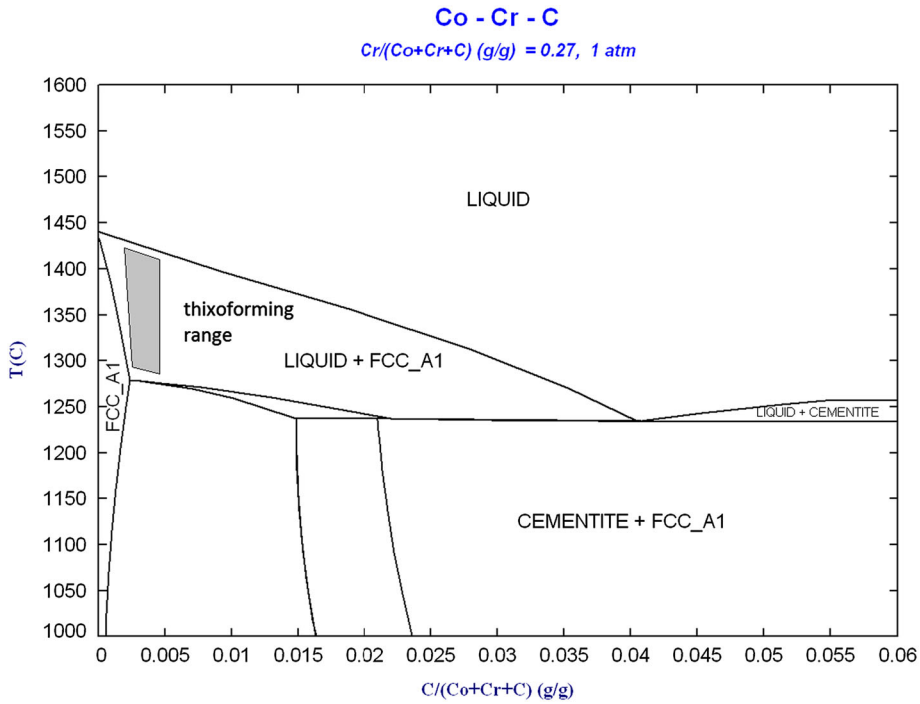

Fig. 1 Co-Cr-C phase diagram with indicated conditions for which thixoforming is possible (for 0.27 wt.% Cr content)

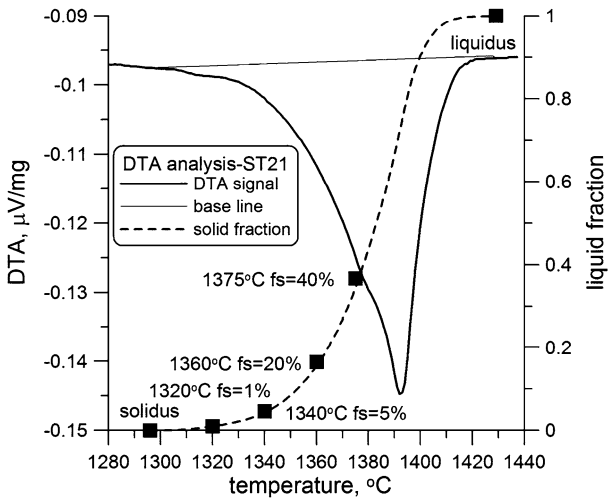

Fig. 2 DTA analysis of Stellite™ 21 alloy with determined liquid fraction (heating rate 5 K/min)

laminar, i.e., very regular, numerical simulation that reproduces the forming of material in the semisolid state has been done quite accurately (Ref 12, 13 and for more information on modeling, see a review Ref 14).

The Stellite™ range of cobalt-chromium alloys are designed for wear and corrosion resistance, and they may also contain tungsten or molybdenum and a small but important amount of carbon. Stellite™ alloys display high hardness and toughness and therefore are very difficult to machine, and anything made from them is, as a result, very expensive. Typically, a Stellite™ part is precisely cast so that only minimal machining is necessary. Stellite™ is more often machined by grinding, rather than by cutting. The alloys also tend to have extremely high melting points due to the cobalt and chromium content. Stellite™ 21 is frequently used in applications in which high temperature wear and chemical attacks can occur. This alloy is also often used in cast form or as a hard-facing material.

X-ray diffraction studies of plastically worked Stellite™ 21 alloy reveal that its microstructure consists of both face-centered cubic (γ(fcc)) and hexagonal close-packed (ε(hpc)) phases. The M_7C_3- and $M_{23}C_6$-type carbides are the predominant minor constituents (where M may be any carbide-forming element, mainly Cr). Furthermore, it was shown that the microstructure of plastically worked alloys forms varying quantities of minor phases, principally in the form of lamellar eutectic, looking like pearlite (Ref 15). The amount of each phase depends on a variety of factors such as alloying elements, stress intensity, heat treatment history, cooling rate, grain size. From a metallurgical point of view, the amount of each phase depends on progress of the martensitic transformation which proceeds, among other things, under mechanical stresses (the strain-induced martensitic transformation). Generally, this transformation plays an important role in controlling material properties such as hardness or susceptibility to mechanical wear (Ref 15-17). The residual, untransformed γ-fcc phase has low stacking fault energy which increases the work hardening ability and consequently, the material hardness. Especially, high amount of γ-Co phase, with increase in temperature, causes higher hardness of the alloy than at room temperature.

The experimental work presented consists of two parts; first the alloy samples were heated to the semisolid state in the specially designed furnace, with precise temperature control, quenched after appropriate heat treatments, followed by detailed examination of the microstructures carried out by (SEM) (EDS) and XRD analyses, and second, investigations into the rheological properties of Stellite™ 21 alloy that would provide crucial information from a technological point of view. Knowledge of the rheological properties is also necessary for numerical modeling of thixoforming processes. In the case of

semisolid slurry, such properties are described by the apparent viscosity. The experimental results were used for development of the mathematical model of Stellite™ 21 alloy viscosity, which could be used directly in numerical simulations.

2. Development of Globular Microstructure in Metal Alloys

Semisolid processing of metal alloys usually consists of two stages: (1) the initial preparation of the feedstock material, usually in the form of a billet, with a near-spheroidal microstructure in the solidus-liquidus range and (2) forming the final near-net-shape product by thixoforging or thixocasting process. A number of methods have been proposed for the preparation of non-dendritic feedstock materials (Ref 14, 19, 20), with the magneto-hydro-dynamic stirring (MHD) method being the most commonly used commercial route for light metal alloys, and sprayforming, although rather expensive clearly applicable for some high value alloys for which other methods do not work. Furthermore, two other methods were developed based on thermo-mechanical treatment of alloys, directly applicable to wrought metal alloys. One is the strain-induced melt-activated (SIMA) method suitable for industrial applications because it is relatively inexpensive and offers an easy way to obtain the non-dendritic feedstock by just heating the highly strained feedstock to the semisolid state. The feedstock is hot-worked material, e.g., rolled, forged or extruded in the solid state above recrystallization temperature and then cooled; such feedstock develops fine globular microstructure after being heated up to the semisolid state. In this study, we used a combination of sprayforming and SIMA methods. It is worth noting that a similar method to the SIMA, the recrystallization and partial melting (RAP) route is another possible way to develop suitable microstructures (Ref 21-23), where the starting material is warm as opposed to hot worked (Fig. 3).

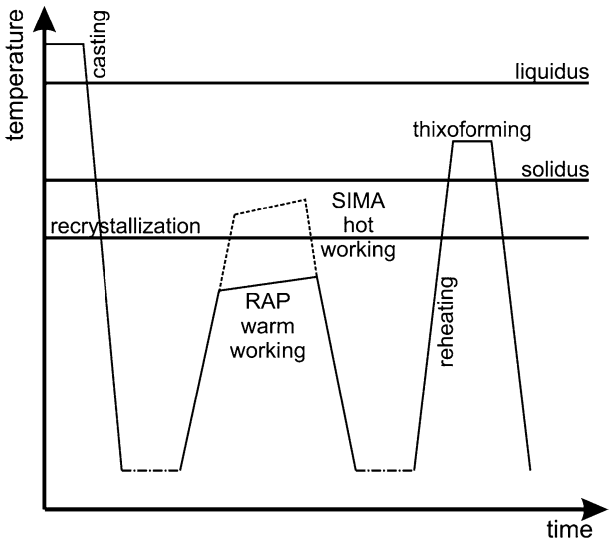

Fig. 3 Schematic illustration of SIMA and RAP processes

3. Experimental Procedure

The first stage of the experimental work involved a high-temperature DTA analysis of the Stellite™ alloy being studied; this analysis was conducted using STA JUPITER 449 analyzer produced by Netzsch. The DTA heating curve and the liquid fraction distribution as a function of temperature for Stellite™ 21 alloy are shown in Fig. 2. The measurements were taken at a heating rate of 5° per minute. It should be indicated that applied heating rate is relatively low in order to obtain conditions close to equilibrium state. In real processes, kinetics of melting process depends on the heating rate which is rather higher than during DTA analysis.

Samples were cut from sprayformed and hot-extruded Stellite™ 21 alloy billets. Their microstructure is shown in Fig. 4, to demonstrate the state of the extruded material. The samples were etched in the mixture of 15 ml of HCl, 10 ml of acetic acid and 10 ml of HNO_3 for 2 min, but this process did not allow the structure resulting from the extrusion process to be clearly observed. Micrographs did not reveal any grain boundaries, but irregular interdendritic and intergranular carbides could be seen, visible as light globules, with an average size of one or two microns; the black parts indicate intergranular lamellar eutectic and the gray the actual grains. The average alloy composition includes (in weight percentage): 61.36%-Co, 27.10%-Cr, 5.69%-Mo, 1.65%-Fe, 2.93%-Ni, 0.59%-Si, 0.25%-C, 0.25%-W, 0.18%-Mn. The microstructural morphology was confirmed on the basis of chemical analysis of selected areas using energy-dispersive spectroscopy (EDS); using FEI E-SEM XL30 with EDS detector EDAX Genesis 4000. These areas are shown in Fig. 5 and the chemical analysis in Table 1. It is easy to recognize that the alloy microstructure of Stellite™ 21 consists of Cr-rich Co solid solution and two types of Cr-rich carbides. The EDS results together with x-ray pattern (Fig. 6) show that the Co solid solution is a mixture of γ-fcc and ε-hcp phases, and two types of carbides Cr_7C_3 and $Cr_{23}C_6$. The Cr_7C_3 carbide is eutectic with the Co solid solution, while the $Cr_{23}C_6$ carbide is a precipitate with fishbone shape.

Samples of approximately 7 × 7 × 10 mm dimensions were suspended on Kanthal wire in a resistance tube furnace and

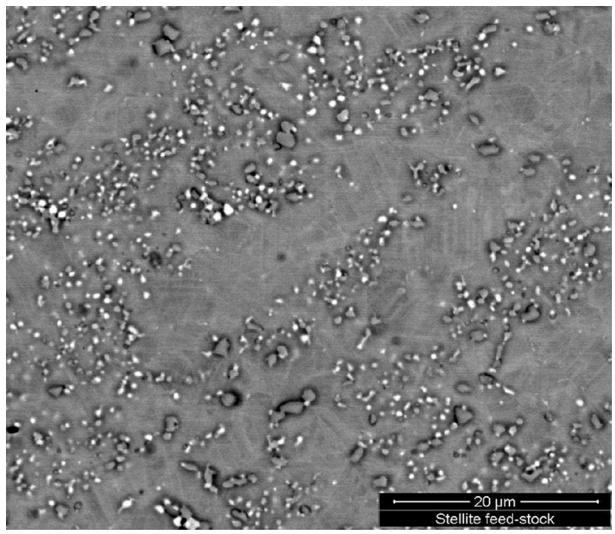

Fig. 4 Scanning microscope microstructure of as-received Stellite™ 21 alloy

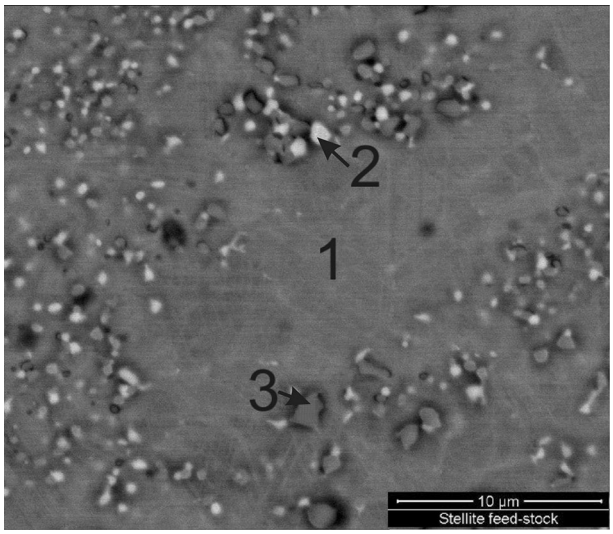

Fig. 5 Selected areas of chemical analysis of the as-received Stellite™ 21 alloy using energy-dispersive spectroscopy (EDS)

heated to a temperature of approximately 1350 °C. To obtain the expected amount of liquid fraction in the semisolid state, the soaking temperatures were taken from the DTA analysis, with temperatures of 1320, 1340, 1360 and 1375 °C corresponding, respectively, to 1%, 5%, 20% and 40% liquid fractions, in accordance with Fig. 2. The samples were soaked at temperature for 10 min and then rapidly quenched in a water tank placed below the furnace. During the heating of the samples, a protective atmosphere of argon gas was used to reduce oxidation. After quenching, the samples were examined by optical and scanning electron microscopy in combination with energy-dispersive spectroscopy. The samples for SEM investigations were polished using diamond powder, and no etching was applied.

4. Effect of Partial Remelting upon the Microstructure of Stellite™ 21 Alloy

The microstructures taken at various temperatures, which correspond to different amount of the liquid phase in the

Table 1 Chemical analysis in selected areas of as-received Stellite™ 21 alloy using energy-dispersive spectroscopy (EDS)

	Element wt.%, at.%							
	Co K	**Cr K**	**Mo L**	**Fe K**	**Ni K**	**Si K**	**C K**	**Total**
1-grain								
wt.%	61.73	26.46	6.34	0.6	2.39	…	2.48	100
at.%	55.71	27.06	3.51	0.57	2.17	…	10.97	100
3-lamellar eutectic								
wt.%	20.03	59.06	11.98	0.24	0.87	…	7.82	100
at.%	14.96	50.01	5.5	0.19	0.65	…	28.68	100
2-carbides								
wt.%	38.31	36.28	19.52	0.44	…	1.28	4.16	100
at.%	33.31	35.75	10.43	0.41	…	2.34	17.76	100

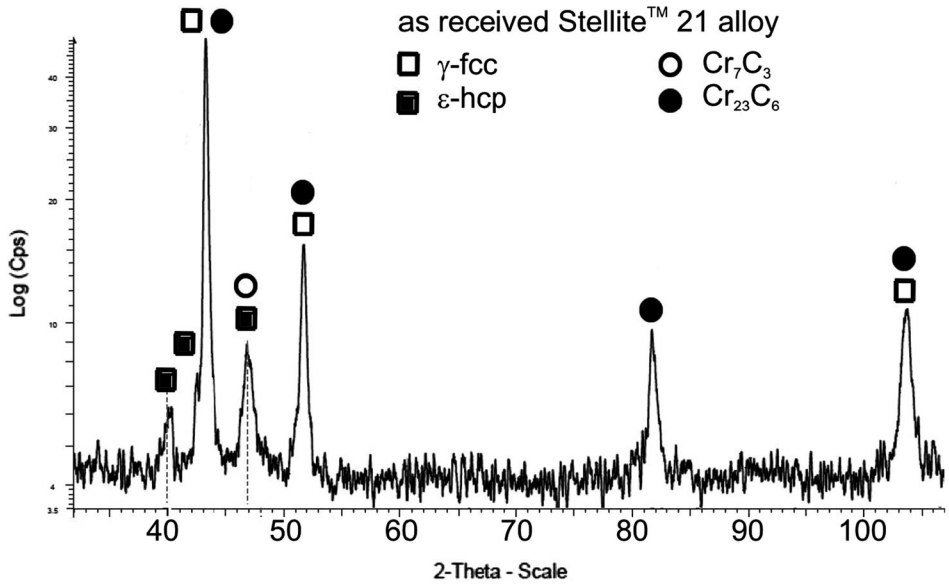

Fig. 6 X-ray diffraction pattern of as-received Stellite™ 21 alloy

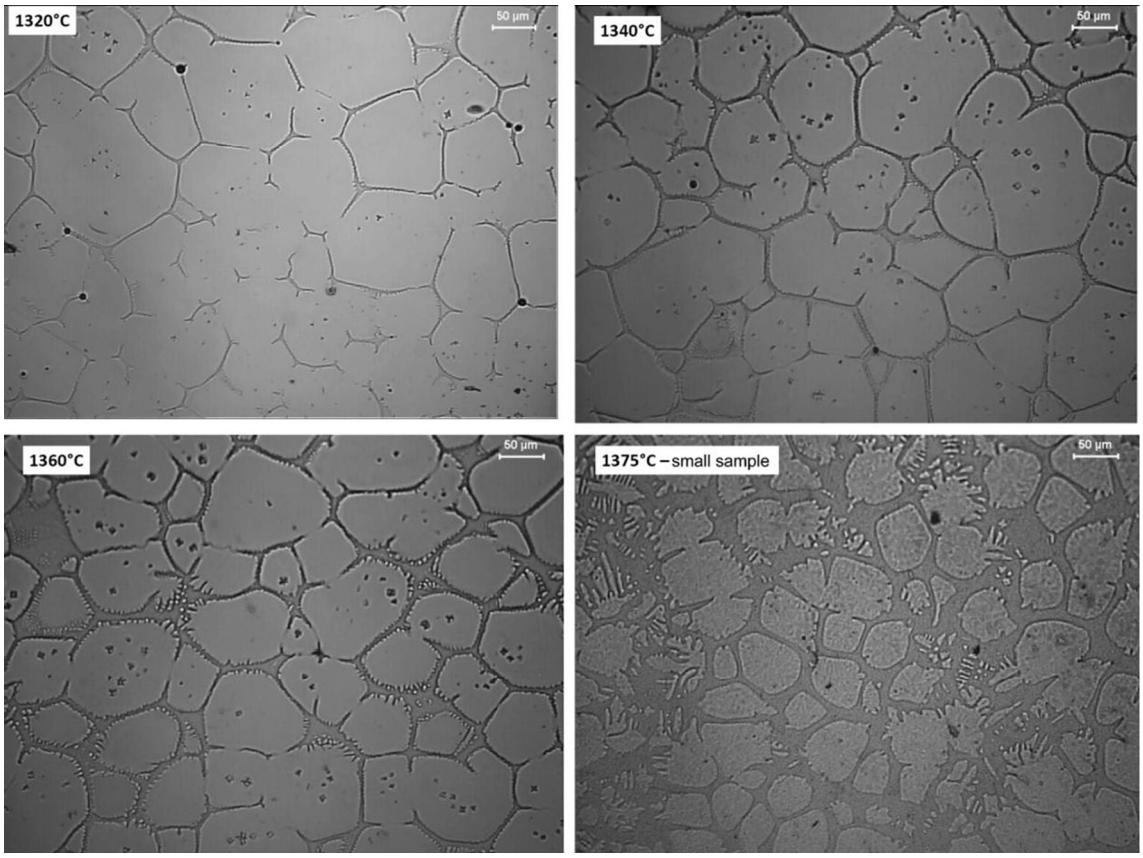

Fig. 7 Microstucture of Stellite™ 21 alloy produced using sprayforming method observed after heating to: 1320, 1340, 1360 and 1375 °C

semisolid state, are shown in Fig. 7. Temperature variations from 1320 to 1375 °C approximately caused variations of liquid fraction from 1 to 40%. The resulting microstructures appear to be composed of regular globular particles embedded in the eutectic formed from the liquid phase, and these microstructures appear suitable for thixoforming. The microstructures were obtained using optical microscopy.

The composition of the material was investigated for both the spheroidal solid particles and their surroundings using the standard EDAX ZAF quantification method, and the results are summarized in Table 2. The areas where composition was analyzed are shown in Fig. 8. They total 100%; however, only elements with a content of over 0.2 wt.% are shown. In both cases, the beam scanned an area of 20 µm × 20 µm, and depth of scanning is assessed as equaling some 1.6 µm, and therefore the measurement gave an average chemical composition in both the globular solid and the low melting phase. No oxygen content was observed inside the globular solid and inside the low melting phase, as determined by means of EDS. These results confirm that oxidation can be avoided during thixoforming of high melting point alloys through appropriate protective gas atmospheres, such as Ar or N_2 (Ref 9). The average composition of the alloy grains after application of the SIMA method is almost the same as grains from as-received material. But the lamellar eutectic is richer in cobalt, mainly due to the higher amount of γ-fcc phase, which occurs under equilibrium conditions. The weight percent of chromium and carbon in area of lamellar eutectic corresponds to stoichiometric Cr_7C_3 carbide. In the sprayformed as-received alloy, the solidification process proceeds under non-equilibrium conditions, and the carbon content does not correspond to the phase diagram.

XRD patterns of Stellite ™ 21 before and after heating have been shown in Fig. 6 and 9. Figure 6 shows that the as-received alloy includes both γ(fcc) and ε(hcp) phases; the γ-Co phase being mainly ⟨111⟩ and ⟨100⟩ textured and the ε-Co phase mainly ⟨0001⟩, ⟨1010⟩ and ⟨1011⟩ textured. The presence of ε-Co phase results from the strain-induced martensitic transformation caused by the extrusion process that the investigated alloy was subjected to. After the heating tests (Fig. 9), the γ-Co phase is mainly observed with fcc structure. The signal of ε-Co phase is very low, which indicates that the strain-induced phase transformation under mechanical stresses proceeded to a small extend. This transformation can occur probably under rapid quenching of samples after aging at high temperatures.

Although the globular microstructure of the material can be examined by optical microscopy, SEM offers higher resolution images, allowing the resolution of individual carbide particles to be achieved, something that cannot be obtained with optical micrographs. Furthermore, additional information on the composition of phases in multicomponent alloys, for which phase diagrams are not easily available, may also be obtained when using EDS. The control of composition is especially critical where samples are subjected to external forces or non-uniform heating.

5. Rheological Properties of Stellite™ 21 Alloy

The rheological analysis was carried out using the high-temperature viscometer FRS 1600, designed by the Anton Paar

Table 2 Chemical analysis in selected areas of annealed at 1320 °C Stellite™ 21 alloy using energy-dispersive spectroscopy (EDS)

	Element wt.%, at.%						
	Co K	Cr K	Mo L	Fe K	Si K	C K	Total
2-grain							
wt.%	64.83	26.90	5.32	0.59	0.99	1.35	100
at.%	60.06	28.24	3.03	0.58	1.93	6.16	100
1-lamellar eutectic							
wt.%	42.97	34.54	18.08	0.33	1.83	2.25	100
at.%	39.63	36.10	10.24	0.32	3.54	10.17	100
3-carbides							
wt.%	38.35	35.91	21.39	0.35	1.59	2.41	100
at.%	35.60	37.79	12.20	0.34	3.11	10.96	100
4-carbides							
wt.%	38.22	35.78	21.90	0.24	1.41	2.46	100
at.%	35.56	37.73	12.51	0.23	2.76	11.21	100

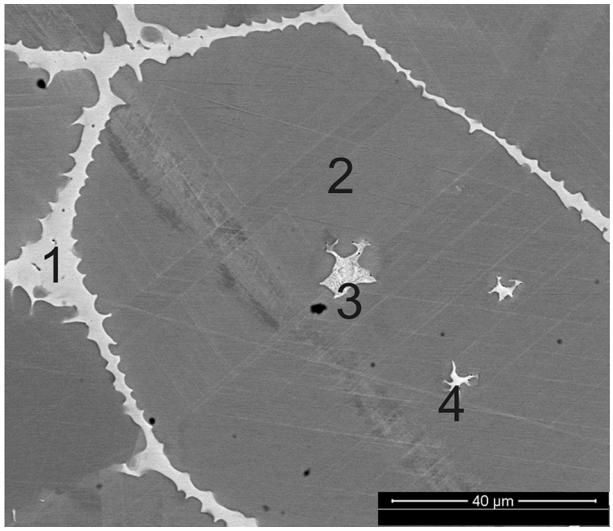

Fig. 8 Selected areas of chemical analysis of annealed at 1320 °C Stellite™ 21 alloy using energy-dispersive spectroscopy (EDS)

company, with a furnace that allows measurements in the temperature range 400-1500 °C. Rheological analysis of Stellite™ 21 alloy in the semisolid state requires work around the 1300-1450 °C temperature range, and the viscosity measurements were performed using Searle's method (Ref 24), carried out using a rotational viscometer with a stationary cup (outer cylinder). In this method, the rod is rotated and the cup is stationary, and the cylinders are concentric, i.e., axi-symmetric with the rotation axis of the inner cylinder. The outer and inner cylinders have 28 and 15 mm in diameter, respectively. They were made from alumina (Al_2O_3). In order to prevent wall slippage on the rotating rod and the crucible, their lateral surfaces have profiled, serrated shape. During experiment, the furnace chamber was blown by the argon gas in order to prevent samples oxidation. Additionally inside furnace chamber, the graphite element was placed to bond rest of oxygen. Before the measurement, the sample was melted to liquid state to place the rotating rod (inner cylinder) inside the crucible (outer cylinder). Next the sample was cooled to assumed temperature, and the viscosity measurement was taken. All the

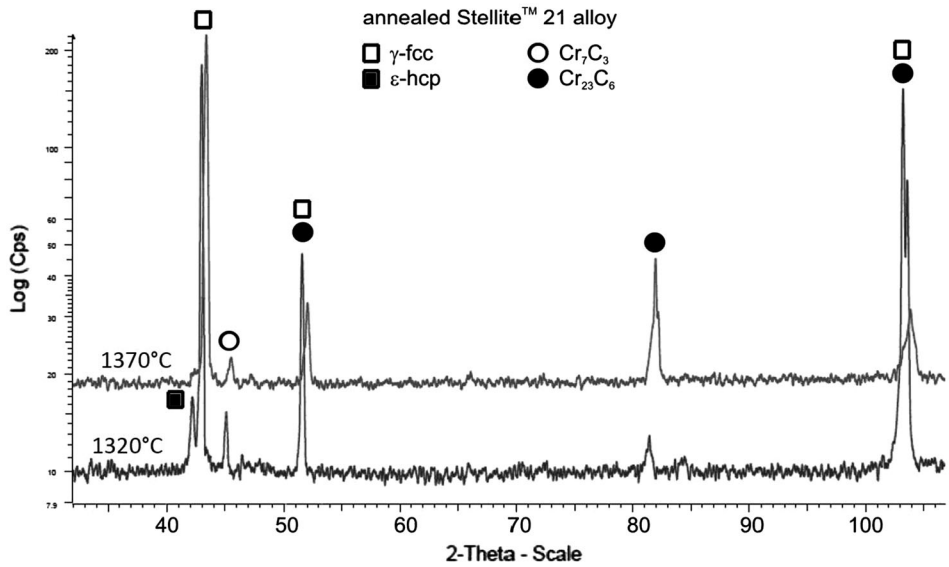

Fig. 9 X-ray diffraction patterns of StelliteTM 21 alloy annealed in semisolid state at temperature of 1320 and 1370 °C

time during temperature changes, the sample was slowly sheared with the rate equals 5 s^{-1}.

As a first step, measurements were concerned with the determination of the relationship between the alloy viscosity and the temperature (Fig. 10). As a basic rule, decrease in temperature causes increase in registered viscosity, especially in the case of metal alloys in the semisolid state. The highest viscosity increase appears for temperatures below 1365 °C. These experiments confirmed results of DTA analysis and allowed to identify the appropriate temperature range for thixocasting of Stellite™ 21 alloy approximately between 1370 and 1390 °C.

In the second step of experimental work an analysis of Stellite™ 21 viscosity in the semi solid state versus the shear rate was carried out. The shear rate ramp was applied in order to control its changes in the range from 0.1 to 20 s^{-1} during measurements. In the range of higher values of the shear rate, the viscosity changes are much less, then in the range of lower

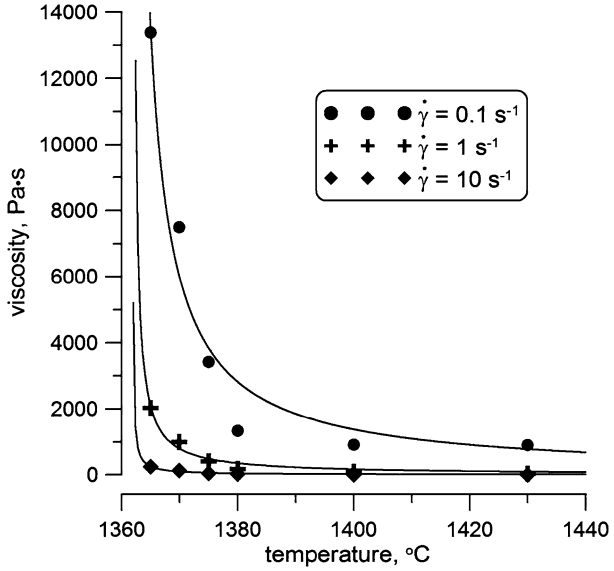

Fig. 10 Relationship between temperature and alloy viscosity

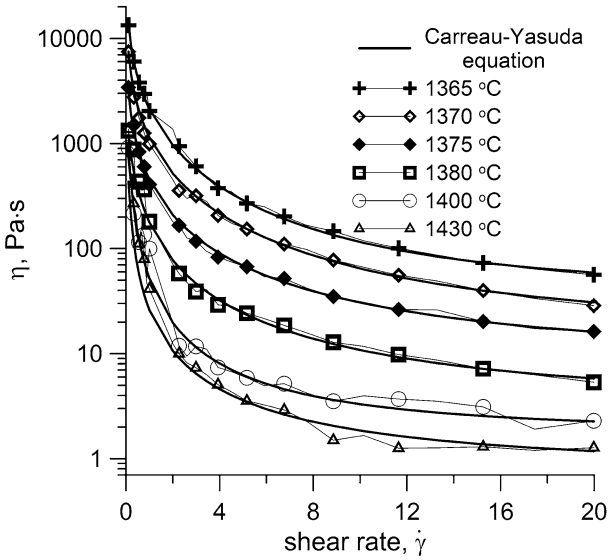

Fig. 12 Curves which approximate (using Carreau-Yasuda model) recorded values of viscosity vs. the shear rate

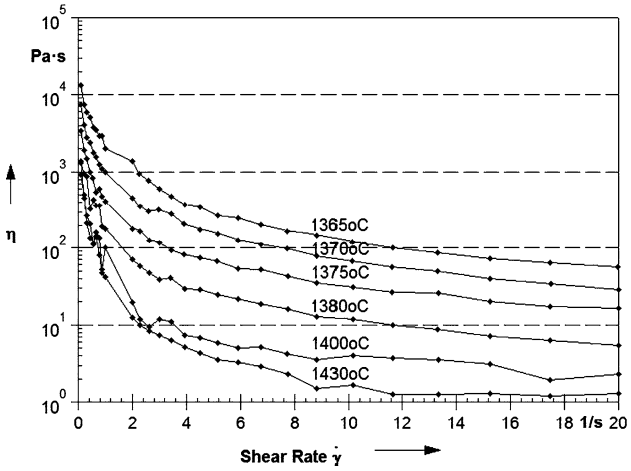

Fig. 11 Viscosity curves of Stellite™ 21 alloy vs. shear rate for selected temperatures in which the semiliquid state appears

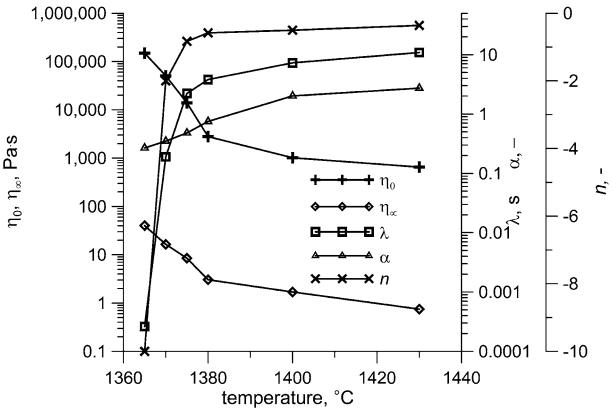

Fig. 13 Parameters values of Carreau-Yasuda viscosity model versus temperature

Table 3 Parameters values of Carreau-Yasuda viscosity model of Stellite™ 21 alloy

Stellite™ 21	η_0, Pa·s	η_∞, Pa·s	λ, s	α	*n*
1365 °C	149,070.40	40.20	0.000262265	0.27	−10.00
1370 °C	50,690.69	16.52	0.19	0.35	−2.00
1375 °C	13,982.20	8.50	2.22	0.48	−0.83
1380 °C	2792.92	3.05	3.81	0.75	−0.58
1400 °C	1016.81	1.70	7.29	2.02	−0.50
1430 °C	652.00	0.75	10.90	2.73	−0.36

values of the shear rate. Moreover, the measurement of viscosity for higher shear rate could follow in the wake of turbulent flow inside the crucible. Figure 11 shows the viscosity curves versus shear rate at the above mentioned temperatures in the semiliquid state for the alloy tested. Before each viscosity measurement, during change in the temperature, the samples were sheared with a rate of about 5 s^{-1}. The temperature changed with rate of 1° per minute. The shape of the curves describing the relationship between the viscosity and the shear rate indicates the shear thinning behavior of the semisolid Stellite™ slurry, i.e., its viscosity decreases with an increasing shear rate.

Numerical simulations, using for example the CDF (*Computational Fluid Dynamics*) method require usually the viscosity models in the form of mathematical equations. One of them is Carreau-Yasuda equation, used very often in the software developed for computer simulations of the casting processes. It should be mentioned that the Carreau-Yasuda equation takes into consideration the shear thinning phenomenon, which occurs in the liquid metals, but this model does not allow the thixotropy phenomenon, which appears in semi-solid alloys, to be described.

$$\eta = \eta_\infty + (\eta_0 - \eta_\infty) \cdot [1 + (\lambda \cdot \dot{\gamma})^{\alpha}]^{\frac{n-1}{\alpha}} \quad \text{(Eq 1)}$$

where $\dot{\gamma}$ is strain rate, η_0 zero strain rate viscosity, η_∞ infinite strain rate viscosity, λ phase shift, n power law coefficient and α Yasuda coefficient.

The obtained parameter values (shown in Table 3) of Eq 1 can be directly applied in the numerical simulations. The approximation was carried out using the gradient optimization method for minimization of differences between measured and calculated viscosity values. The correctness of the approximation of the viscosity curves could be observed in Fig. 12. The values of Carreau-Yasuda parameters versus temperature are also shown in Fig. 13.

6. Conclusions

The study has verified that using sprayforming for the preparation of feedstock billets for thixoforming is a promising route for obtaining the prerequisite globular microstructure in Stellite™ 21 alloy.

The use of scanning electron microscopy in combination with energy-dispersive spectroscopy provides valuable insights into the microstructural details normally associated with semisolid alloy feedstock.

No oxygen was observed to be present in either the globular solid or in the low melting phase. Oxidation was avoided by the application of argon gas atmosphere as observed by other authors (Ref 9), pointing to the fact that industrial thixoforming of high melting point alloys should be carried out in a protective gas atmosphere.

EDS analysis revealed concentration of carbides in the liquid phase of Stellite™ 21 alloy sample heated to the semisolid state at 1320 °C.

Strain-induced transformation in Stellite™ 21 happened at high temperatures as can be seen in the XRD pattern obtained for samples heated at high temperatures after extrusion. Generally, such transformation leads to the formation of ε-Co phase from γ-Co phase. Temperature is another important parameter responsible for this transformation, and XRD patterns of the as-received and re-heated alloy show that the relative fraction of γ-Co phase decreases with temperature increases. Higher amount of γ-Co phase, especially at high temperatures, causes increase in alloy hardness, indicating possible uses for special applications.

Analysis of the apparent viscosity showed the susceptibility of this alloy to forming in the semisolid state. The alloy has a wide enough solidification range and low enough viscosity to allow this kind of shaping technique to be a potential practical application. The rheological tests carried out show that the Stellite™ 21 alloy in the semiliquid state acts as a non-Newtonian fluid, with viscosity strongly dependent on shear rate. The relationship between these two parameters corresponds to shear thinning behavior, and in this state, the viscosity is very sensitive even to small changes in temperature.

Acknowledgments

Research financed through statutory funds of AGH University of Science and Technology in Krakow, No. 11.11.110.225.

Open Access

This article is distributed under the terms of the Creative Commons Attribution 4.0 International License (http://creativecommons.org/licenses/by/4.0/), which permits unrestricted use, distribution, and reproduction in any medium, provided you give appropriate credit to the original author(s) and the source, provide a link to the Creative Commons license, and indicate if changes were made.

Appendix

This paper is the eleventh publication from a thematically related series from the process of conferment of the degree of doktor habilitowany to Dr. Krzysztof Sołek, pursuant to the rules laid down in the Act of 14 March 2003 on Academic Degrees and Title and Degrees and Title in the Arts with later changes (Republic of Poland law). This series concerns the thixoforming of high melting point metal alloys (exampled Ref 6, 18). Generally, these investigations were focused on the development of globular microstructure, the measurement and modeling of alloys rheological properties and the shaping of semisolid metal alloys (steel and Stellite™ alloys). This paper is devoted to development of globular microstructure in Stellite™ 21 alloy and analysis of its viscosity.

References

1. D.B. Spencer, R. Mehrabian, and M.C. Flemings, Rheological Behaviour of Sn-15% Pb in the Crystallization Range, *Metall. Trans.*, 1972, **3**, p 1925–1932
2. D. Walukas, S. LeBeau, N. Prewitt, and R. Decker, Thixomolding®—technology opportunities and practical uses, *Proceedings of 6th International Conference on Semi-Solid Processing of Alloys and Composites*, G.L. Chiarmetta and M. Rosso, Ed., Edimet Spa, Brescia, 2000, p 109–114
3. K. Young and P. Eisen, SSM technological alternatives for different applications, *Proceedings of 6th International Conference on Semi-*

Solid Processing of Alloys and Composites, G.L. Chiarmetta and M. Rosso, Ed., Edimet Spa, Brescia, 2000, p 97–102
4. P. Kapranos, Semi-Solid Metal Processing – A Process Looking for a Market, *Solid State Phenom.*, 2008, **141–143**, p 1–8
5. S.C. Hogg, H.V. Atkinson, and P. Kapranos, Thixoforming of Stellite Powder Compacts, *Proceedings of 10th ESAFORM Conference On Material Forming*, E. Cueto and F. Chinesta, Ed., AIP Publishing LLC, Zaragoza, 2007, p 1191–1198
6. J. Dutkiewicz, Ł. Rogal, K. Sołek, and A. Mitura, Thixoforming Technology of High Carbon X210CrW12 Steel, *Int. J. Mater. Form*, 2009, **2**(Suppl 1), p 753–756
7. S.Y. Lee and S.Y. Lee, Comparative Evaluation of TiN/CrN, AlN/CrN, TiAlN/CrN Multilayer Films for the use of Semi-Solid Processing of Cu Alloys, *Solid State Phenom.*, 2006, **116–117**, p 124–127
8. R. Telle, S. Muenstermann, and C. Beyer, Design, Construction and Performance of Silicon Nitride Tool Parts in Steel Thixoforming, *Solid State Phenom.*, 2006, **116–117**, p 690–695
9. B.A. Behrens, D. Fisher, B. Haller, A. Rassili, J.C. Pierret, H. Klemm, A. Studinski, B. Walkin, M. Karlsson, M. Robelet, L. Natale, and F. Alpini, Series Production of Thixoformed Steel Parts, *Solid State Phenom.*, 2006, **116–117**, p 686–689
10. M.C. Flemings and R.A. Martinez, Principles of Microstructural Formation in Semi-Solid Metal Processing, *Solid State Phenom.*, 2006, **116–117**, p 1–8
11. H.A. Barnes, Thixotropy—A Review, *J. Non Newtonian Fluid Mech.*, 1997, **70**, p 1–33
12. K. Sołek, T. Stuczyński, A. Białobrzeski, R. Kuziak, and Z. Mitura, Modelling Thixocasting with Precise Accounting of Moving Front of Material, *Mat. Sci. Tech.*, 2005, **215**, p 551
13. K. Sołek, Z. Mitura, R. Kuziak, and P. Kapranos, The use of ADINA Software to Simulate Thixocasting Processes, *Solid State Phenom.*, 2006, **116–117**, p 626–629
14. H.V. Atkinson, Modelling the Semisolid Processing of Metallic Alloys, *Prog. Mater Sci.*, 2005, **50**, p 341–412
15. F.J. Clauss, J.W. Weeton, Effect of Heat Treatment Upon the Microstructure and Hardness of a Wrought Cobalt-Base Alloy, Stellite 21. NACA TN 3107, 1954
16. H. Kashani, A. Amadeh, and A. Ohadizadeh, Effect of Temperature on the Strain Induced $\gamma \rightarrow \varepsilon$ Phase Transformation in Stellite 21 During Wear Test, *Mater. Sci. Eng. A*, 2006, **435–436**, p 474–477
17. I. Radu, D.Y. Li, and R. Llewellyn, Tribological Behavior of Stellite 21 Modified with Yttrium, *Wear*, 2004, **25**, p 1154–1166
18. J. Dutkiewicz, Ł. Rogal, K. Sołek, Z. Mitura, and P. Kapranos, Thixoforming of Spray Formed M2 Tool Steel, *Int. J. Mater. Form*, 2010, **3**, p 755–758
19. P. Kapranos and D.H. Kirkwood, Thixoforming M2 Tool Steel: A Study of Different Feedstock Routes, *La Metallurgia Italiana*, 2010, **9**, p 17–21
20. P. Kapranos, Semi-Solid Processing of High Melting Point Materials: Feedstock Routes. *Encycl. Iron Steel Alloys*, 2014
21. D. Liu, H.V. Atkinson, and P. Kapranos, Structural evolution by RAP and thixoforming of wrought alloy 2014, *Proceedings of 5th International EASAFORM Conference on Material Forming*, M. Pietrzyk, Z. Mitura, and J. Kaczmar, Ed., Publishing House Akapit, Kraków, 2002, p 667–670
22. M. Robelet, A. Rassili, and D. Fischer, Steel Grades Adapted to the Thixoforging Process: Metallurgical Structures and Mechanical Properties, *Solid State Phenom.*, 2006, **116–117**, p 712–716
23. G. Vaneetveld, A. Rassili, and H.V. Atkinson, Influence of Parameters during Induction Heating Cycle of 7075 Aluminium Alloys with RAP Process, *Solid State Phenom.*, 2008, **141–143**, p 719–724
24. G.T. Mezger, *The Rheology Handbook: For Users of Rotational and Oscillatory Rheometers*, 2nd revised edition, Vincentz Network, Hannover, 2006, p 171–198